10

Optical and luminescent properties of $MgAl_2O_4$ ceramics doped with high level of Eu^{3+} ions concentrations

© D.T. Valiev, O.L. Khasanov, E.S. Dvilis, V.D. Paygin, C. Lin, S.A. Stepanov¶

Tomsk Polytechnic University, Tomsk, Russia

¶e-mail: stepanovsa@tpu.ru

Received December 09, 2022
Revised January 09, 2023
Accepted January 11, 2023

The series of $MgAl_2O_4$ ceramics doped with high level of europium oxide (Eu_2O_3) up to 15 wt.% was fabricated by the Spark Plasma Sintering technique. The prepared ceramics have been tested using the various experimental techniques: X-ray diffraction, scanning electron microscopy, as well as optical and cathodoluminescence spectroscopy. The influence of europium oxide on the complex of optical and luminescent characteristics of 1300°C ceramics is discussed. The nature of the luminescence centers and the luminescence decay parameters are considered in detail.

Keywords: $MgAl_2O_4$ spinel ceramics, europium oxide, Spark Plasma Sintering, luminescence.

DOI: 10.61011/EOS.2023.05.56505.53-22

1. Introduction

High-density aluminum-magnesium spinel ceramic ($MgAl_2O_4$, MAS) has a unique combination of mechanical, optical and thermal properties, high melting point, chemical and abrasion resistance [1,2]. It is a promising material for replacing single crystals and glasses, since it has clearly expressed advantages over the latter. The technology for the manufacture of optically transparent ceramics is devoid of the main disadvantages of traditional methods of growing single crystals and obtaining glass, which are the long duration of the processes, the necessity to purify materials, and the availability of complex technological equipment [1–3]. Transparent materials based on $MgAl_2O_4$ are used in aviation, rocketry and space technology; elements of optical telescopes, passive optics, output windows of ultraviolet and infrared laser devices operating in extreme conditions are made from it [1–5].

In recent decades, there has been increasing interest in the study of polycrystalline aluminum-magnesium spinel as a luminescent material. In papers [6–9], the luminescent properties of spinel activation by transition metals, and in papers [10–13] by rare-earth ions, were studied. The opportunity of obtaining transparent luminescent MAS-ceramics with different content of Yb_2O_3 [14] was demonstrated, the optical-luminescent characteristics of MAS-ceramic with additions of CeO_2 and Eu_2O_3 [15,16], Tb_4O_7 and Dy_2O_3 [17,18] were studied, the thermoluminescence of MAS-ceramics with Eu_2O_3 content up to 1 mas.% [19] was studied.

From practical application point of view, europium oxide is a promising additive – activator, since the Eu^{3+} ions contained in it have $^5D_0 \rightarrow {}^7F_J$ ($J = 0, 1, 2, 3, 4$) transitions and are widely used as activators in the manufacture of light sources, indicator devices and displays [20–26].

To manufacture the luminescent MAS-ceramics, the most common methods are hot pressing or Spark Plasma Sintering (SPS). The latter is more promising. The duration of sintering by this method does not exceed tens of minutes, as a result of which the growth of grains is minimal, and their sizes inherit the sizes of particles of sintered powders. In the process of SPS, a uniform distribution of density occurs in the volume of sintered ceramics, and perfect grain boundaries are formed [27].

One of the ground problems in the manufacture of transparent luminescent MAS-ceramics is the low solubility of rare-earth oxides in the aluminum-magnesium spinel matrix, which leads to the formation of impurity (secondary) phases and degradation of optical properties [14]. The solution to this problem can be the use of high-quality nanopowders as raw materials [8], efficient methods of mixing and consolidating powder mixtures.

In this work, we demonstrate the possibility of obtaining fluorescent ceramics based on $MgAl_2O_4$ with a high concentration of europium oxide by pulsed electric current sintering. The influence of high concentrations of europium oxide on the optoluminescent characteristics of ceramics has been studied.

2. Examined samples and experimental procedure

2.1. Manufacture of ceramics $MgAl_2O_4$, activated by Eu_2O_3

For the preparation of ceramic samples, mixtures of powders of aluminum-magnesium spinel (SC30R, Baikowski, France) and europium oxide (Nevatorg, Russia) were prepared. Mixing was carried out in isopropyl alcohol using a ball mill for 48 h, then the powders were calcined at a

temperature of 70°C until the liquid completely evaporated. The concentration of europium oxide in powder mixtures was 0.01, 0.1, 1, 5, 15 wt.%.

The powder was consolidated on an SPS 515S Spark plasma sintering machine (SyntexInc, Japan) in a vacuum (10^{-3} Pa) at a temperature of 1300°C under a pressure of 100 MPa. The duration of isothermal exposure at a given sintering temperature was 20 min.

Cylindrical ceramic samples with a height of 2 mm and a diameter of 14 mm were obtained as a result of sintering. To perform further studies, the obtained samples were sequentially ground and polished on an EcoMet-300 unit (Buehler, Germany). After mechanical processing, the height of the samples was 1.5 mm.

2.2. Experimental methods

X-ray diffraction (XRD) analysis was performed on an XRD-7000S diffractometer (Shimadzu, Japan). The survey was carried out with CuKα radiation in the range from 25° to 90° by 2θ with a step of 0.02°. The resulting diffraction patterns were interpreted by the Rietveld method using the free software „PowderCell“ and the international crystallographic database „PDF 4“.

The study of the optical properties of the samples in the ultraviolet, visible and near infrared areas was carried out using a two-beam scanning spectrophotometer SF-256UVI (200–1100 nm).

A GIN-400 electron accelerator was used to excite pulsed cathodoluminescence. The duration of the electron pulse at half-width was 12 ns, the average energy of accelerated electrons was 240 keV. The sample was placed in a vacuum chamber. The cathodoluminescence decay kinetics was recorded using an PMT-97 photomultiplier using an MDR-12 monochromator (spectral range 200–2000 nm, linear dispersion 1.3 nm/mm) and a Tektronix DPO3034 digital oscilloscope (300 MHz). The recording of integrated PCL emission spectra „per pulse“ was carried out by an AvaSpec-2048 fiber-optic spectrometer (340–1100 nm). The emission spectra were corrected for the spectral sensitivity of the optical path.

3. Results

3.1. Structure and X-ray diffraction analysis

Aluminum-magnesium spinel has a face-centered cubic crystal lattice. Anions are located at the lattice sites, which form a dense cubic packing. Cations are located in interstices and partially fill them. The coordination polyhedron for the magnesium cation is — a tetrahedron. The coordination polyhedron for the aluminum cation is — a octahedron. Thus, the spinel structure consists of octahedra and tetrahedra and has two different cation sublattices, and each anion belongs to one tetrahedron and three octahedra. The chemical bond in the aluminum-magnesium spinel is mixed — ionic-covalent. Depending on the distribution of cations in the interstices, spinels are divided into three types: normal, inverted, and mixed.

From the point of view of practical application, aluminum-magnesium spinel is very attractive, since aluminum Al^{3+} and magnesium Mg^{2+} cations occupying opposite positions [28] can play the role of trapping centers and enhance the luminescence intensity [19].

When europium oxide is introduced into aluminum-magnesium spinel, europium ions Eu^{3+} primarily replace the tetrahedral positions of magnesium cations. This is due to a smaller difference in their ionic radii than the difference in the ionic radii of europium and aluminum [29,30]. The same happens with europium ions Eu^{2+} [25]. Moreover, with an increase in the europium concentration in aluminum-magnesium spinel, Eu^{2+} ions can occupy octahedral positions of aluminum cations [19].

X-ray diffraction patterns of MAS:Eu samples are demonstrated in Fig. 1. The resulting ceramics consists of a cubic aluminum-magnesium spinel. On the diffraction patterns of samples with a calculated content of europium oxide up to 1 mas.%, peaks characteristic of europium oxide compounds were not recorded. This is due to limitations of the XRD analysis method.

Peaks characteristic of the compound $EuAlO_3$ (PDF #000-30-0012) were recorded in samples with a calculated concentration of europium oxide of 5 and 15 mas.%. The quantitative content of $EuAlO_3$ is 3.9 and 11.8% for samples with 5 and 15 mas.% Eu_2O_3, respectively. In addition, low-intensity peaks characteristic of MgO were found in the diffraction patterns for all concentrations, which indicates the formation of this compound in trace amounts.

The results of the evaluation of the phase composition and structural parameters: crystal lattice parameter (a), average CSR size (D), crystal lattice microstresses (ε) are shown in Fig. 1, *b* , *c, d*. As a result of sintering, an 4–10-fold increase in the size of the CSR is observed in comparison with the initial powder. With an increase in the concentration of Eu_2O_3 from 0 to 15 mas.%, the average CSR sizes change in the range from 166 to 366 nm, the crystal lattice microstresses change in the range from 0.000108 to 0.000245. The smallest value of CSR and the largest value of microstrains of the crystal lattice is demonstrated by the sample containing 5 mas.% Eu_2O_3.

An analysis of the structural morphology of the MAS:Eu samples, based on the results of SEM on the cleavage surface (Fig. 2), revealed a predominantly transcrystalline fracture pattern of the studied ceramic, indicating high strength and quality of grain boundaries.

The average ceramic grain size at the level of 850 nm remained in the submicron range. The size of grain boundaries did not exceed 1 nm. There are both grains of the ground phase and the impurity phase in the images obtained in the phase contrast mode. Their number increases with an increase in the calculated concentration of europium oxide.

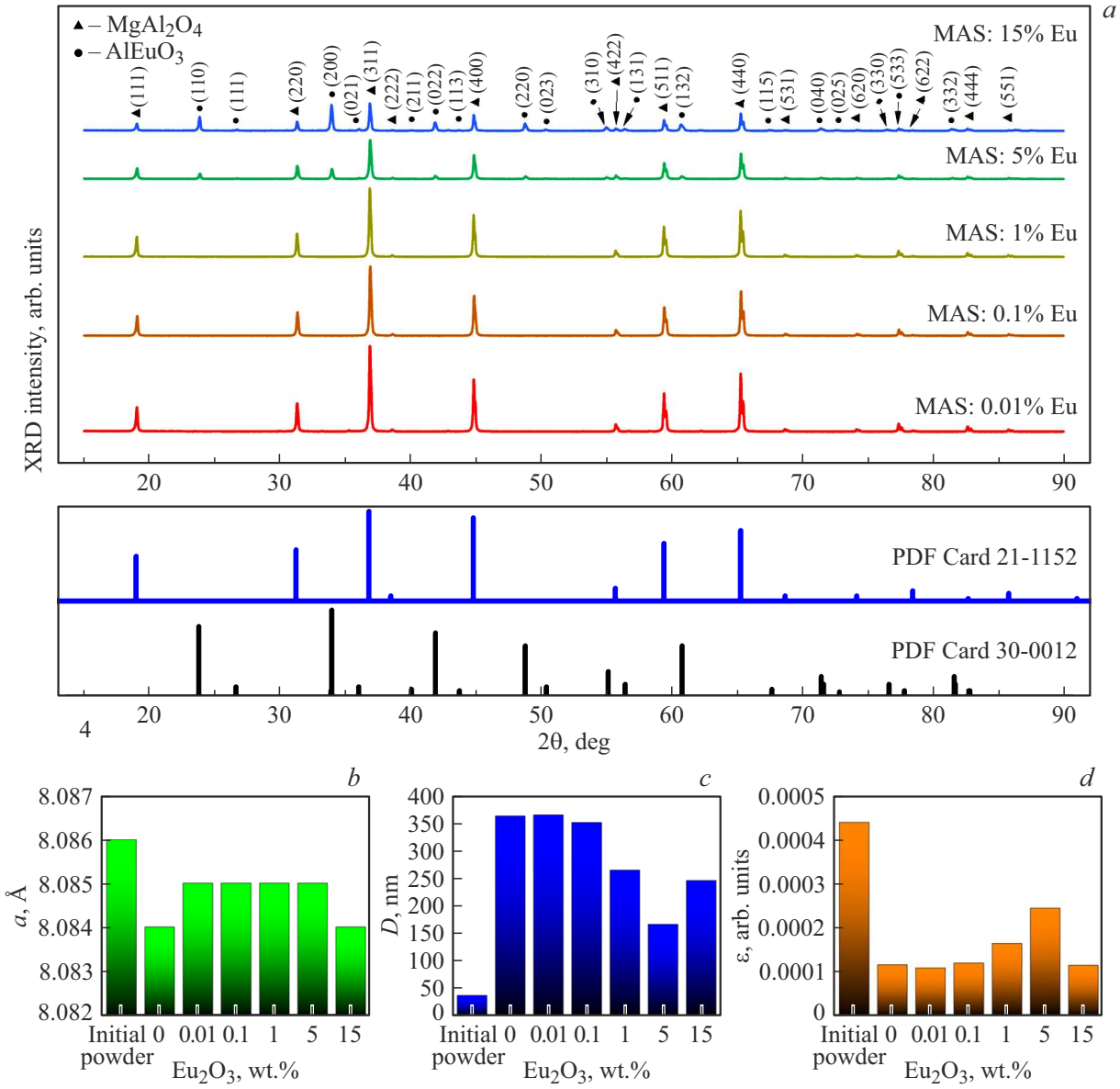

Figure 1. X-ray diffraction patterns of samples (a) and crystal lattice parameters of ceramics (b, c, d) $MgAl_2O_4$: $x\%Eu_2O_3$.

3.2. Optical and luminescent properties

Fig. 3 shows the transmittance spectra of ceramic samples based on aluminum-magnesium spinel with a variable concentration of europium oxide. From the obtained results, it can be noted that ceramic samples with low concentrations of europium oxide (< 1 mas.%) have higher values of the transmittance in the spectral range 500–1100 nm. The highest transmittance is approximately 70% in the near-IR area for the MAS sample: 0.01% Eu. Increasing the concentration of europium oxide to 1 mas.% and higher leads to a decrease in the values of the transmission coefficient, while the transmission boundary is shifted by 650 nm. Apparently, this is due to the formation of a new phase of europium aluminate (Fig. 3, *a*).

After annealing at a temperature of 1300°C, there is a general decrease in the transmission across the spectrum (Fig. 3, *b*). So, for a wavelength of 500 nm for the MAS sample: 0.01% Eu transmittance from 40% before annealing decreased to 10% after annealing. In the IR range, the value of the transmittance is consistent with the samples before annealing and decreases with increasing europium oxide concentration, starting 5%.

Fig. 3, *c, d* shows cathodoluminescence spectra. Before annealing, with an increase in the europium concentration, an increase in the integrated radiation intensity is observed (see inset in Fig. 3, *c*). The emission consists of a wide luminescence band in the 340–600 nm area, due to the intrinsic luminescence centers of the *F*-type [15]. In this spectral area, there is also a luminescence band of the

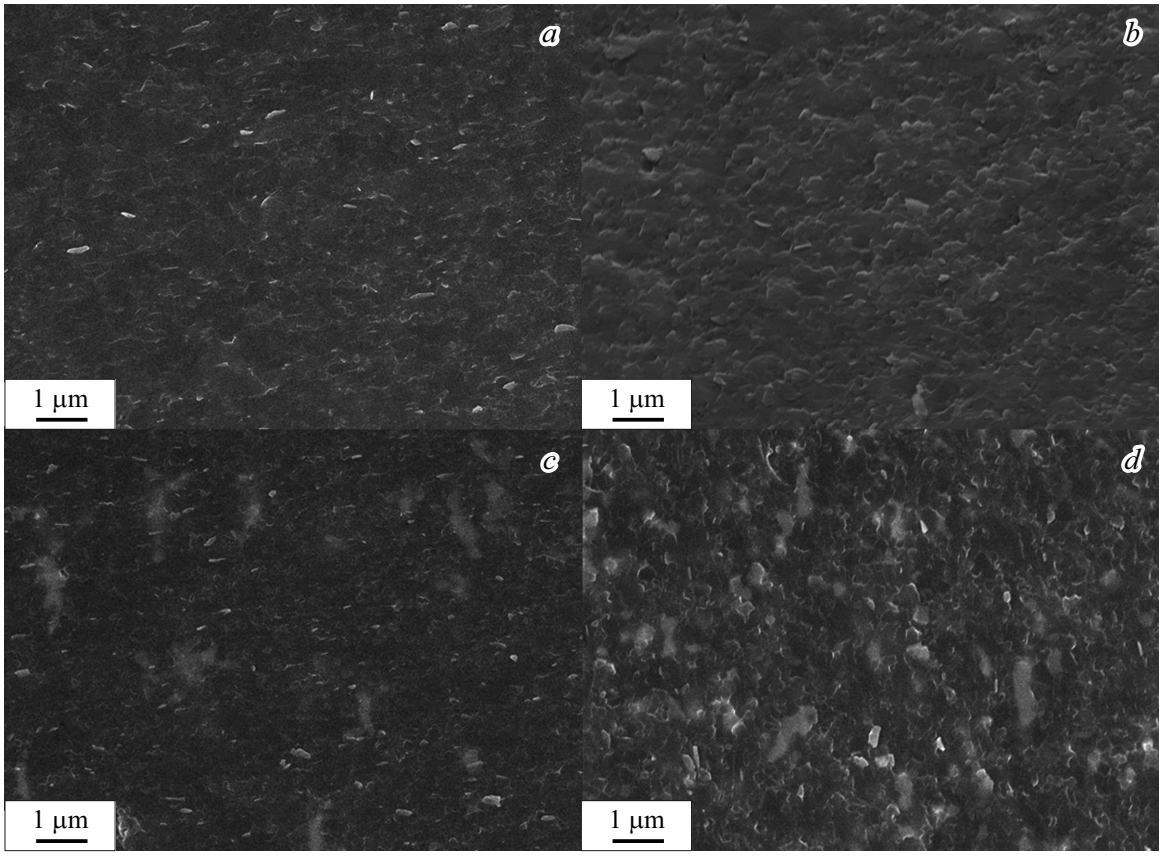

Figure 2. SEM images of the cleavage surface of the obtained ceramic samples MAS:0.01%Eu (*a*), MAS:1%Eu (*b*), MAS:5%Eu (*c*), MAS:15%Eu (*d*).

$5d-4f$ transition of the Eu^{2+} ion with a maximum at 460 nm [19,25], due to the substitution of the Mg cation in the tetrahedral position. The intensity of this glow band increases with an increase in the concentration of europium oxide up to 1 mas.% (Fig. 3, *c*). Increasing the concentration of europium oxide to 5 and 15 mas.% leads to a sharp decrease in the band at 460 nm and the appearance of a narrow band with a maximum at 614 nm, due to the Eu^{3+} ion of $EuAlO_3$ phase.

A band at 520 nm is also recorded in the luminescence spectra, and a change in the concentration of europium oxide has practically no effect on this emission band. In the papers [19,31,32] this glow is attributed to the $^4T_1$ (4G)-$^6A_1$ (6S) transition of Mn^{2+} impurity ions. We could not confirm the presence of this impurity. Meanwhile, this glow is in good agreement with the emission of *F* centers of MgO [33,34]. Further, in the area of the spectrum 650−800 nm (Fig. 3, *c*), a broad band is recorded with a maximum in the area of 700 nm, due to Mg^{2+} vacancies [19,32]. Several narrow bands (maximum peak at 688 nm) are superimposed on this wide band, due to the luminescence of the chromium ion [9,15]. The impurity glow of chromium remains almost constant with changes in the concentration of europium oxide. Meanwhile, there is a sharp increase in the intensity of the luminescence band by 700 nm, due to Mg^{2+} vacancies, with an increase in the concentration of europium oxide to 5 and 15 mas.%. We attribute this increase in intensity to the formation of a new $EuAlO_3$ phase and, as a consequence, an increase in the concentration of Mg $^{2+}$ vacancies.

After annealing, the spectral composition of the radiation does not change (Fig. 3, *d*), however, the dependence of the integrated luminescence intensity on the concentration of europium oxide changes to the opposite (Fig. 3, *d* insert). This is due to a general change in the contribution of the emission bands and a significant increase in the intensity of the emission band by 520 nm. This cumulative effect of annealing on the emission bands at 520 nm (*F*-MgO centers) and 700 nm (Mg^{2+} vacancies) can be associated with the formation of a higher concentration of local inclusions of the MgO phase. Unfortunately, the low total concentrations of the MgO phase in the samples do not allow to confirm such changes upon annealing by other methods. The ground factor influencing the decrease in the luminescence intensity with an increase in the concentration of europium oxide is the occupation of the Mg tetrahedral sites with europium. This leads both to a decrease in the concentration of Mg^{2+} vacancies and, accordingly, to a decrease in the luminescence in the area of the 700 nm [19,32] band, and to a decrease in the emission

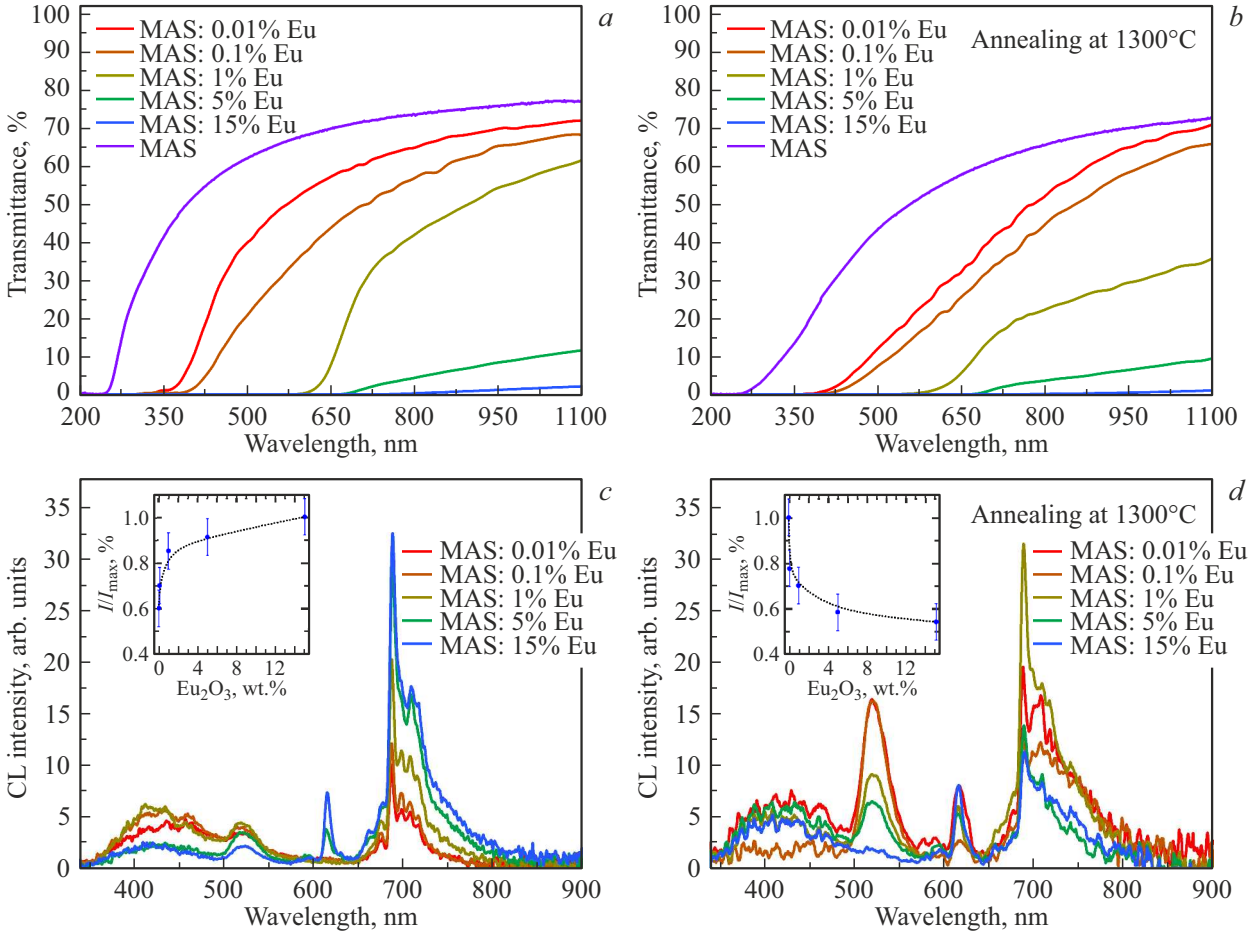

Figure 3. Total transmission spectra before annealing (*a*) and after atmospheric annealing at a temperature 1300°C (*b*). Cathodoluminescence spectra before annealing (*c*) and after annealing (*d*).

intensity in the luminescence band by 520 nm (*F* are centers of MgO [33,34]).

The luminescence decay kinetics of MAS:Eu ceramics are shown in Fig. 4.

The luminescence at a wavelength of 412 nm, the nature of which is due to the luminescence of the spinel matrix and the luminescence of the Eu^{2+} ion, is described by the sum of two exponential functions (Fig. 5, *a*). The characteristic times in this area correspond to the components 40 and 500 ns on average (Fig. 5, *a*). Three attenuation components can be distinguished (Fig. 5, *b*) for the luminescence band with a maximum of 520 nm. Meanwhile, the characteristic decay times $\tau_1 \sim 0.18$ ms and $\tau_3 \sim 10$ ms do not depend on the europium concentration, while τ_2 sharply increases with an increase in the europium oxide concentration to 5 mas.% from 2.4 to 3.5 ms (Fig. 5, *b*).

The luminescence band at 614 nm is also described by the sum of three exponential functions (Fig. 5, *c*). The characteristic time $\tau_3 \sim 26$ ms does not change with an increase in the europium concentration, and τ_1 and τ_2 also increase abruptly with an increase in the concentration of europium oxide up to 5 mas.% from 0.18 to 0.67 ms and from 1.5 to 3.2 ms (Fig. 5, *c*) respectively. This change seems to be associated with the formation of the $EuAlO_3$ phase. The luminescence responsible for the emission transitions in the chromium ion at a wavelength of 688 nm is described by the sum of two exponents: the first component is $\tau_1 \sim 3.5$ ms, the second is $\tau_2 \sim 42$ ms (Fig. 4, *d*).

Conclusion

Ceramics based on aluminum-magnesium spinel activated with europium oxide was successfully synthesized by Spark plasma sintering. Transparency and cathodoluminescent properties were studied. The transmittance of ceramics decreases with increasing concentration of europium oxide. Ceramics with 15 mas.% europium oxide has the highest radiation intensity before annealing, and after annealing, due to a multiple increase in luminescence in the 520 nm band, ceramics with a content of 0.01 mas% europium oxide show maximum radiative characteristics. Accordingly, for ceramics without annealing, the optimal concentrations of europium oxide for transparency and radiation intensity do not coincide, while after annealing 0.01 mas.% of europium is the optimal concentration both from the position of trans-

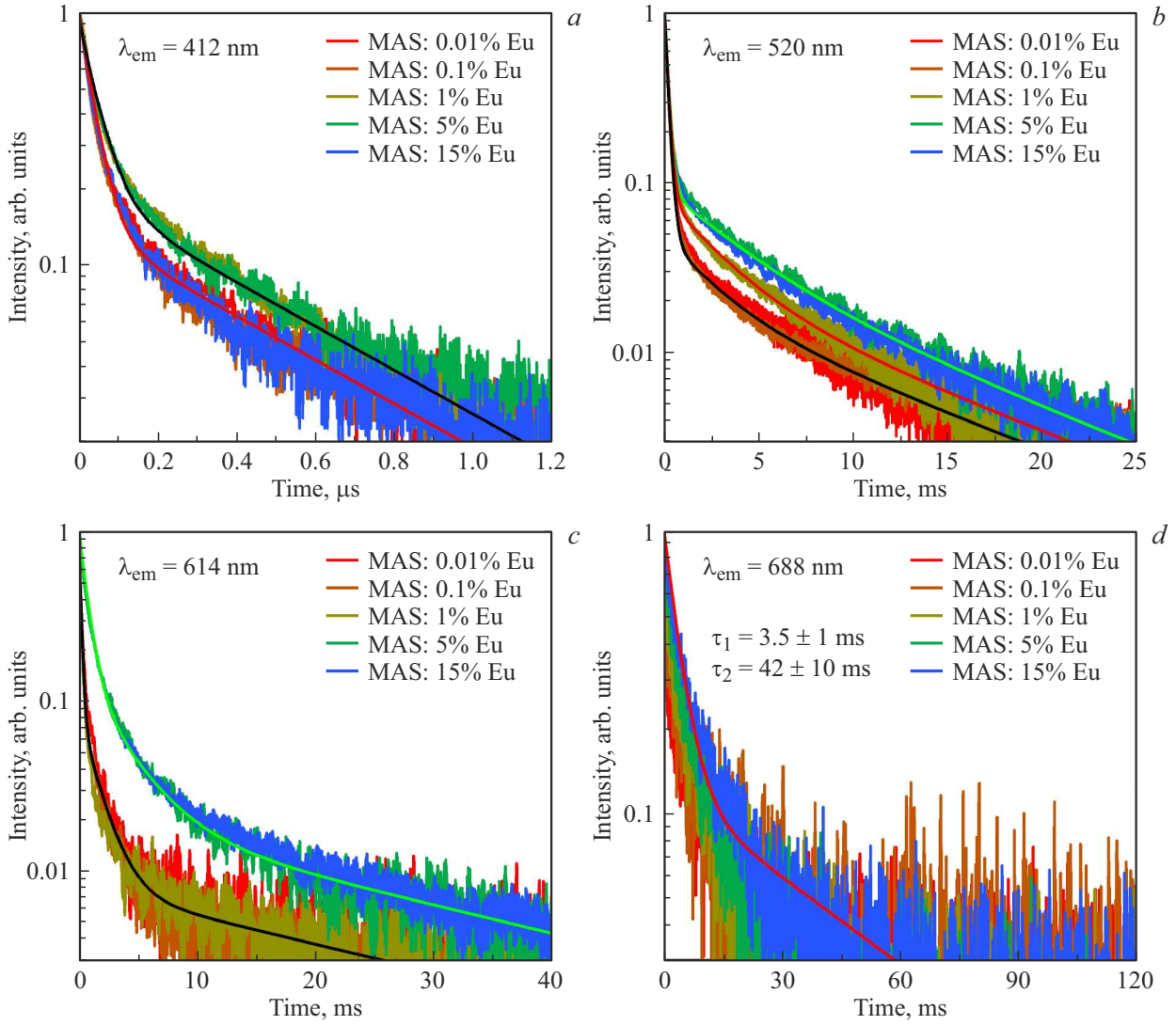

Figure 4. Kinetic characteristics of radiation of samples $MgAl_2O_4:Eu$.

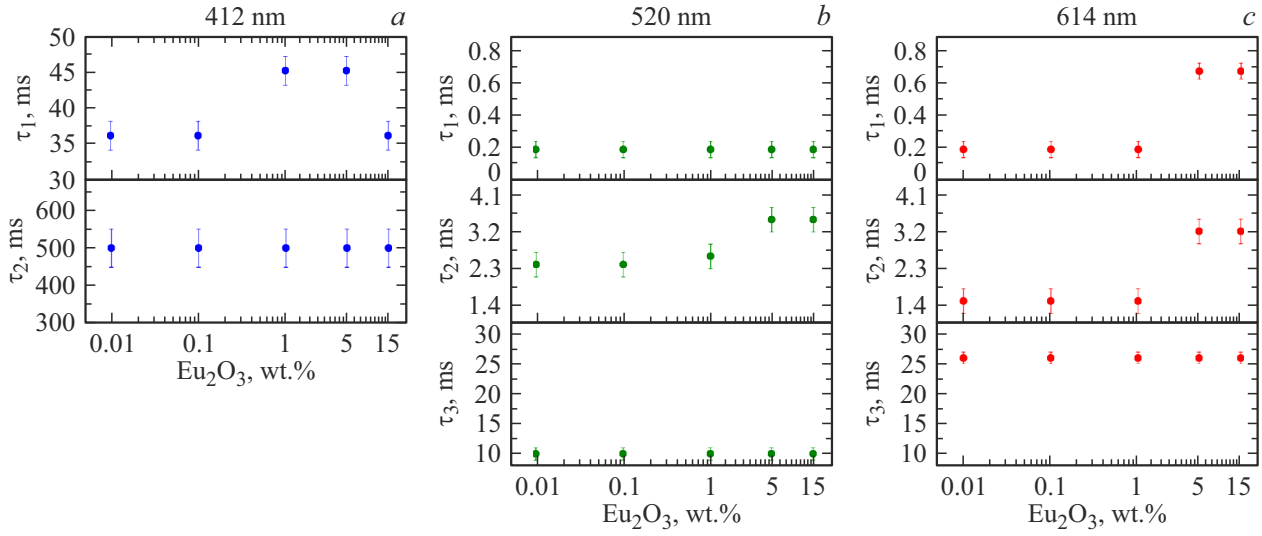

Figure 5. Characteristic decay times of radiation $MgAl_2O_4:Eu$.

parency and from the position of luminescence intensity. The nature of the radiation of the obtained ceramic materials is due to the intrinsic luminescence centers of the *F*-type in the area up to 600 nm with superimposed luminescence bands at 460 nm of the Eu^{2+} ion and at 520 nm of the *F*-MgO centers. In the near IR area, the luminescence is due to Mg^{2+} vacancies and impurity radiation of the Cr^{3+} ion. A change in the concentration of europium oxide affects the filling of tetrahedral Mg positions and, accordingly, allows to control the ratio of the luminescence bands of the resulting material. It should also be noted that it is possible to control the luminescence intensity of individual spectral bands (in the 520, 614, and 688 nm area) of the material obtained using atmospheric annealing in wide ranges.

Funding

This study was financially supported by the Russian Science Foundation (project № 21-73-10100. In the paper, the equipment of the Centre for Collective Use CSU NMNT TPU supported by the project of the Ministry of Education and Science of Russia № 075-15-2021-710, was used.

Conflict of interest

The authors declare that they have no conflict of interest.

References

[1] A. Goldstein. J. European Ceramic Society, **32** (11), 2869 (2012). DOI: 10.1016/j.jeurceramsoc.2012.02.051
[2] Z. Shi, Q. Zhao, B. Guo, T. Ji, H. Wang. Materials & Design, **193**, 108858 (2020). DOI: 10.1016/j.matdes.2020.108858
[3] Q. Sai, C. Xia, H. Rao, X. Xu, G. Zhou, P. Xu. J. Luminescence, **131** (11), 2359 (2011). DOI: 10.1016/j.jlumin.2011.05.046
[4] X. Liu, X. Qian, P. Zheng, Z. Hu, X. Chen, H. Pan, J. Zou, R. Xie, J. Li. J. European Ceramic Society, **39** (15), 4965 (2019). DOI: 10.1016/j.jeurceramsoc.2019.07.027
[5] Z. Wang, H. Ji, J. Xu, X. Hou, J. Ueda, S. Tanabe, S. Yi, Y. Zhou, D. Chen. Inorganic Chemistry, **59** (24), 18374 (2020). DOI: 10.1021/acs.inorgchem.0c03005
[6] L. Basyrova, V. Bukina, S. Balabanov, A. Belyaev, V. Drobotenko, O. Dymshits, I. Alekseeva, M. Tsenter, S. Zapalova, A. Khubetsov, A. Zhilin, A. Volokitina, V. Vitkin, X. Mateos, J.M. Serres, P. Camy, P. Loiko. J. Luminescence, **236**, 118090 (2021). DOI: 10.1016/J.JLUMIN.2021.118090
[7] L. Nataf, F. Rodríguez, R. Valiente, V. Ulanov. J. Luminescence, **129** (12), 1602 (2009). DOI: 10.1016/j.jlumin.2008.12.030
[8] N.V. Kuleshov, V.G. Shcherbitsky, V.P. Mikhailov, S. Kück, J. Koetke, K. Petermann, G. Huber. J. Luminescence, **71** (4), 265 (1997). DOI: 10.1016/S0022-2313(96)00284-0
[9] N. Mironova-Ulmane, M.G. Brik, J. Grube, G. Krieke, A. Antuzevics, V. Skvortsova, M. Kemere, E. Elsts, A. Sarakovskis, M. Piasecki, A.I. Popov. Optical Materials, **121**, 111496 (2021). DOI: 10.1016/j.optmat.2021.111496
[10] E.A. Raja, S. Menon, B. Dhabekar, N.S. Rawat, T.K. Gundu Rao. J. Luminescence, **129** (8), 829 (2009). DOI: 10.1016/j.jlumin.2009.03.001
[11] Y. Takebuchi, H. Fukushima, D. Nakauchi, T. Kato, N. Kawaguchi, T. Yanagida. J. Luminescence, **223**, 117139 (2020). DOI: 10.1016/j.jlumin.2020.117139
[12] T. Kato, D. Nakauchi, N. Kawaguchi, T. Yanagida. Optik, **207**, 164433 (2020). DOI: 10.1016/j.ijleo.2020.164433
[13] R.J. Wiglusz, T. Grzyb, A. Lukowiak, P. Głuchowski, S. Lis, W. Strek. Optical Materials, **35** (2), 130 (2012). DOI: 10.1016/j.optmat.2012.07.017
[14] S.S. Balabanov, A.V. Belyaev, E.M. Gavrishchuk, I.B. Mukhin, A.V. Novikova, O.V. Palashov, D.A. Permin, I.L. Snetkov. Optical Materials, **71**, 17–22 (2017). DOI: 10.1016/j.optmat.2016.10.033
[15] D. Valiev, O. Khasanov, E. Dvilis, S. Stepanov, E. Polisadova, V. Paygin. Ceramics International, **44** (17), 20768–20773 (2018). DOI: 10.1016/j.ceramint.2018.08.076
[16] C.-F. Chen, F.P. Doty, R.J.T. Houk, R.O. Loutfy, H.M. Volz, P. Yang. J. American Ceramic Society, **93**, 2399–2402 (2010). DOI: 10.1111/j.1551-2916.2010.03721.x
[17] D. Valiev, S. Stepanov, O. Khasanov, E. Dvilis, E. Polisadova, V. Paygin. Optical Materials, **91**, 396–400 (2019). DOI: 10.1016/j.optmat.2019.03.049
[18] D. Valiev, O. Khasanov, E. Dvilis, S. Stepanov, V. Paygin, A. Ilela. Phys. Status Solidi B, **257**, 1900471 (2020). DOI: 10.1002/pssb.201900471
[19] T. Kato, D. Nakauchi, N. Kawaguchi, T. Yanagida. J. Luminescence, **251**, 119136 (2022). DOI: 10.1016/j.jlumin.2022.119136
[20] Z. Wang, S. Jiao, Y. Xu, Q. Zhang, Y. Chen, G. Pang, S. Feng. J. Luminescence, **211**, 108 (2019). DOI: 10.1016/j.jlumin.2019.03.008
[21] N.T. Chi, N.V. Quang, N.T. Tuan, N.T. Kien, D.Q. Trung, P.T. Huy, P.D. Tam, D.H. Nguyen. J. Electronic Materials, **48** (9), 5891 (2019). DOI: 10.1007/s11664-019-07358-5
[22] S.V. Motloung, B.F. Dejene, O.M. Ntwaeaborwa, H.C. Swart, R.E. Kroon. Chemical Physics, **487**, 75 (2017). DOI: 10.1016/j.chemphys.2017.02.009
[23] I. Beketov, A.I. Medvedev, O.M. Samatov, A.V. Spirina, K.I. Shabanova. J. Alloys and Compounds, **586**, S472 (2014). DOI: 10.1016/j.jallcom.2013.02.070
[24] S.V. Motloung, B.F. Dejene, R.E. Kroon, O.M. Ntwaeaborwa, H.C. Swart, T.E. Motaung. Optik, **131**, 705 (2017). DOI: 10.1016/j.ijleo.2016.11.165
[25] K. Waetzig, I. Kinski. Zeitschrift für Naturforschung B, **69** (2), 159 (2014). DOI: 10.5560/znb.2014-3277
[26] W. Guan, J. Li, X. Wang. Physica Status Solidi (a), **211** (8), 1778 (2014). DOI: 10.1002/pssa.201431268
[27] S.F. Wang, J. Zhang, D.W. Luo, F. Gu, D.Y. Tang, Z.L. Dong, G.E.B. Tan, W.X. Que, T.S. Zhang, S. Li, L.B. Kong. Progress in Solid State Chemistry, **41** (1–2), 20–54 (2013). DOI: 10.1016/j.progsolidstchem.2012.12.002
[28] E.M. Yoshimura, E.G. Yukihara. Radiation Measurements, **41** (2), 163–169 (2006). DOI: 10.1016/j.radmeas.2005.09.001.
[29] I. Kolesnikov, E.V. Golyeva, A.V. Kurochkin, M. Mikhailov. J. Alloys and Compounds, **654**, 32 (2016). DOI: 10.1016/j.jallcom.2015.09.122
[30] I.E. Kolesnikov, E.V. Golyeva, E.V. Borisov, E.Yu. Kolesnikov, E. Lähderanta, A.V. Kurochkin, M.D. Mikhailov. J. Rare Earths, **37** (8), 806 (2019). DOI: 10.1016/j.jre.2018.10.019

[31] A. Tomita, T. Sato, K. Tanaka, Y. Kawabe, M. Shirai, K. Tanaka, E. Hanamura. J. Luminescence, **109** (1), 19–24 (2004). DOI: 10.1016/j.jlumin.2003.12.049
[32] Mu-Tsun Tsai, Yee-Shin Chang, Ing-Bang Huang, Bo-Yu Pan. Ceramics International, **39**, 3691 (2013). DOI: 10.1016/j.ceramint.2012.10.201
[33] C. Ballesteros, J. Piqueras, J. Llopis. MRS Online Proceedings Library, **24**, 229–232 (1983). DOI: 10.1557/PROC-24-229
[34] C. Ballesteros, J. Piqueras, J. Llopis, R. González. Physica Status Solidi (a), **83** (2), 645–649 (1984). DOI: 10.1002/pssa.2210830229

Translated by E.Potapova